Dynamic Nuclear Polarization of Liquids in Very Weak Fields

Don D. Thompson, Robert J. S. Brown, and Richard J. Runge

California Research Corporation, La Habra, California

The validity of the modified Bloch equations (MBE) for liquids in extremely weak dc magnetic fields and large values of electron spin saturation, using linear rf fields, has been checked for anthracene-negative-ion solutions (ANI). Strictly numerical solutions of the MBE were obtained by use of a computer to show the electron spin saturation as functions of rf field strength and frequency. These functions were strongly non-monotonic and exceed unity in some cases. Dynamic nuclear polarizations were measured by a low-field transient method in which proton free-precession was observed in a weak field. Conventional epr measurements at 3000 and 18 G, cw dynamic nuclear polarization measurements at 18 G, and the low-field transient dynamic nuclear polarization measurements were all compatible with $T_1 = T_2 = T = 50$ nsec for the ANI at 29°C. The ratio k of nuclear polarization enhancement to the electron spin saturation was found to be very nearly constant, in agreement with the Solomon two-spin relaxation theory. By use of MBE with $T = 50$ nsec and setting $k = -162$, the results of the dynamic nuclear polarization measurements were fit to very nearly within known experimental errors despite the wide range of low-field resonant and nonresonant conditions and the strongly nonmonotonic curves. No dynamic polarization of the ANI could be obtained with the rf field parallel to the dc field, in agreement with the MBE. However, a crude-oil-derived free radical with $T_1 > T_2 \approx 10$ nsec yielded about one-third as large a dynamic nuclear polarization with the rf field parallel to the dc field as perpendicular. It was noticed for a deteriorated ANI sample that the time constant for the establishment of a dynamic nuclear polarization exceeded the proton relaxation time and also varied markedly with the strength of the rf field.

I. INTRODUCTION

A THEORETICAL and experimental study of the low-field dynamic nuclear polarization of liquids produced by linearly polarized rf fields has been undertaken in order to test the validity of the low-field modified Bloch equations[1-3] (MBE), as well as the two-spin relaxation theory of Solomon[4] in the extreme low-field limit. During the course of this investigation, work by Hecht,[5] Hecht and Redfield,[6] and Jerome and Galleron[7] on the low-field Overhauser effect in Na and Li metals was published, and many of their results pertinent to ours were corroborated. We have found that the dynamic nuclear polarization in a liquid may be calculated in terms of a single adjustable parameter by use of numerical solutions of the MBE. As was first found by Hecht,[5] the electron saturation δ_S was obtained from solutions of the MBE for small H_0 and a strong linearly polarized rf field, $H_{rf} = 2H_1$, was *not* a monotonic function of H_{rf}.

The solutions of the MBE for a circularly polarized rf field was given by Whitfield and Redfield,[8] and the formulas for M_{ZR}, χ_R', and χ_R'' were exhibited in closed form. M_{ZR} is the Z component of the macroscopic electron spin magnetization, and χ_R' and χ_R'' are the real and imaginary parts of the complex rf susceptibility produced by the rotating field. There exist no such known solutions for the large linear field case.

Several samples were studied, but we shall report here a typical one, namely, anthracene negative ion (ANI) dissolved in tetrahydrofuran. The electron resonance of this solution was studied both at 3000 and 18 G. The resonance displays a nearly perfect Lorentzian line with the spin-spin relaxation time T_2 equal to 50 nsec at both fields.

The dynamic polarization data were taken by the free-precession technique of Packard and Varian[9] except that, during the polarization cycle, rf power was applied to the sample. The rf-induced nuclear enhancement was negative and very large, ranging up to 150 under some conditions.

A theoretical study of the low-dc-field electron saturation δ_S of a free radical is given, extending the findings of Hecht[5] to much lower dc fields. The results indicate an interesting frequency dependence of δ_S. Included also is a brief discussion of the calculated behavior of the imaginary part of the rf susceptibility χ'', showing its variation with rf field strength from the Bloch ($2H_1/H_0 \ll 1$) to the Debye ($2H_1/H_0 \gg 1$) limits.

II. THEORY

The MBE for the electrons with which we are concerned is

$$\frac{d\mathbf{M}}{dt} + \frac{\mathbf{M}}{T_2} + \left(\frac{1}{T_1} - \frac{1}{T_2}\right)\left(\frac{\mathbf{M}\cdot\mathbf{H}}{H^2}\right)\mathbf{H} - \gamma\mathbf{M} \times \mathbf{H} = \frac{\chi_0 \mathbf{H}}{T_1}, \quad (1)$$

where $\mathbf{M}$ is the electron macroscopic magnetization, $\mathbf{H}$ is the *total* field and is given in the linearly polarized case by

$$\mathbf{H} = (H_{rf}\cos\omega t, 0, H_0). \quad (2)$$

[1] R. S. Codrington, J. D. Olds, and H. C. Torrey, Phys. Rev. 95, 607 (1954).
[2] M. A. Garstens and J. I. Kaplan, Phys. Rev. 99, 459 (1955).
[3] R. J. Runge, J. Math. Phys. 3, 1267 (1962).
[4] I. Solomon, Phys. Rev. 99, 559 (1955).
[5] R. Hecht, Phys. Rev. 132, 966 (1963).
[6] R. Hecht and A. G. Redfield, Phys. Rev. 132, 972 (1963).
[7] D. Jerome and G. Galleron, Phys. Chem. Solids 24, 1557 (1963).
[8] G. Whitfield and A. G. Redfield, Phys. Rev. 106, 918 (1957).
[9] M. Packard and R. Varian, Phys. Rev. 93, 941 (1954).

In Eq. (1), γ is the magnetogyric ratio of the free electrons, and χ_0 is the static value of the electron susceptibility. The steady-state solutions of Eq. (1) to be later presented are based upon numerical methods given by Runge.[3] All of the approximate methods tried, such as the low-harmonic solution,[3] yielded curves which could not be fitted with any degree of accuracy to the experimental data over the complete range of variation of H_{rf}.

In the case of a linearly polarized rf field, such as the x component in Eq. (2), it was necessary to solve Eq. (1) for cases of high saturation

$$\gamma^2 H_1^2 T_1 T_2 > 1 \qquad (3)$$

by numerical techniques. What was done was to begin with an initial choice of $\mathbf{M}$ and numerically forward integrate Eq. (1) until transient effects had disappeared and a periodic solution resulted. We chose $\mathbf{M}$ to be initially zero and forward integrated 10 rf cycles at time steps Δt equal to 1/100 the rf period. At the end of the forward integration, i.e., on the tenth rf cycle, $\mathbf{M}$ was carefully inspected to see if it was indeed periodic. Then a recalculation at double timestep was performed to verify the accuracy of the numerical solutions. In all cases exhibited below, periodicity was verified to 1 part in 10^5, and the accuracy of the solution was better than a part in 10^4 discrepancy between the original and double timestep calculations. Decay of transients to e^{-2} of their original value occurred in times of the order of 300 nsec or less. The smallest rf period involved, i.e., for 14 Mc/sec, was 71.5 nsec; hence, forward integration out to 10 rf cycles was adequate in reducing transients to the vanishing point. Thus, the last cycles of the solutions were steady state.

By a minor modification of the computer program given by Runge,[3] we were able to compute $M_z(t)$. The time average $\langle M_z \rangle_{av}$ was then computed by a numerical integration of $M_z(t)$ over the last rf cycle. This integration was a straightforward staircase integration and was quite accurate for our small Δt. The electron saturation δ_S was defined as

$$\delta_S = (\chi_0 H_0 - \langle M_z \rangle_{av})/\chi_0 H_0. \qquad (4)$$

Since $\langle M_z \rangle_{av}$ was used only in Eq. (4), χ_0 for the electron was taken as equal to unity for convenience. In addition to the M_z calculations, we computed χ'', the imaginary part of the rf susceptibility. For this purpose, the relation

$$2\omega H_1^2 \chi'' = \frac{1}{\tau} \int_0^\tau \mathbf{H} \cdot \frac{d}{dt} \mathbf{M} dt \qquad (5)$$

was used.

For the electron-proton interaction, the Solomon[4] relation (with constant, H_0- and H_{rf}-independent relaxation times) may be written, in our notation, as

$$\delta_I = k\delta_S, \qquad (6)$$

where δ_I is the nuclear enhancement obtained from the

measured quantities I_0, I_z and the relationship

$$\delta_I = (I_z - I_0)/I_0. \qquad (7)$$

I_0 and I_z are the static and dynamic nuclear polarizations, respectively. In Eq. (6), k is a factor whose sign is determined by the nature of the electron-nuclear interaction (in this case, negative). Its magnitude depends on many environmental factors, such as temperature or the whiteness of the "noise" spectrum the nucleus sees; however, its maximum magnitude is 330 for a dipolar interaction. The dc field dependence of the Overhauser effect in metals, which was the subject of Abragam's[10] study, need not concern us here, because effective local fields in liquids are small. The assumptions used here are valid as long as $\omega\tau_c \ll 1$, where τ_c is the correlation time for molecular motion; this condition was well satisfied in our experiments.

We attempt to relate the experimental data by Eqs. (4), (6), and (7) with k as the only parameter other than electron relaxation time to be determined by experiment.

III. BEHAVIOR OF MBE IN NONRESONANT REGION

Since no formulas for δ_S or χ''/χ_0 have been exhibited in closed form for highly saturated, low-frequency cases, we decided to explore some aspects of the variation of these quantities with ω and H_1 by making numerical calculations for the hypothetical but reasonable case of a liquid in which $T_1 = T_2 = T = 60$ nsec for the electron relaxation times. This represents an exchange-narrowed free-radical with linewidth of about 1 G.

In Fig. 1, δ_S is shown as a function of $H_{rf}(= 2H_1)$ for a dc field $H_0 = 0.5$ G. Three curves are shown for rf frequencies $f = 3.5$, 7.0, and 14.0 Mc/sec. Each curve rises from $\delta_S = 0$ at $H_{rf} = 0$, following a dependence on H_{rf} which is at first monotonic and well represented by a δ_S obtainable from the low-harmonic approximate solutions[3] to the MBE for a linearly polarized rf field. At a value $|\gamma| H_{rf}/\omega \approx 2$, δ_S reaches a maximum, and it oscillates as H_{rf} is increased further. The period of oscillation $\Delta H_{rf} \approx 3\omega/|\gamma|$. The function is apparently oscillatory for $\omega T \gtrsim 1$. Increasing ωT from 2.5 to 5 does
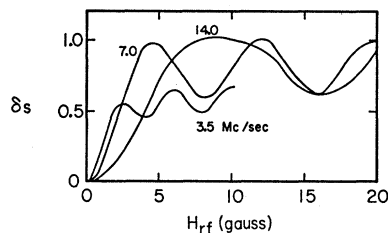

FIG. 1. Curves computed from modified Bloch equation showing the electron spin saturation δ_S as functions of rf field strength $H_{rf} = 2H_1$ for rf frequencies of 3.5, 7.0, and 14.0 Mc/sec, a dc field strength $H_0 = 0.5$ G, and $T_1 = T_2 = T = 60$ nsec.

[10] A. Abragam, Compt. Rend. 254, 3848 (1962).

not appear to increase the peak-to-valley ratio appreciably.

In Fig. 2, χ''/χ_0 is shown for this case except that H_0 is here increased to 2.5 G, the resonant field for $f=7$ Mc/sec, and the behavior of χ''/χ_0 versus H_{rf} is shown in going from $H_{rf}=0$ to $H_{rf}=12$ G. This range covers the extremes, $H_{rf}/H_0\ll1$ (Bloch case) and $H_{rf}/H_0\gg1$ (Debye case).

At resonance, the Bloch equation gives for χ''/χ_0 the value (for $H_{rf}\ll H_0$)

$$(\chi''/\chi_0)_{\text{Bloch}}=\tfrac{1}{2}\omega_0 T_2=1.32.$$

For $H_{rf}\gg H_0$, the Debye result is

$$(\chi''/\chi_0)_{\text{Debye}}=\omega T_1/(1+\omega^2 T_1^2)=0.33,$$

for our values of H_0, $|\gamma|$, T_1, T_2, and ω.

Figure 2 thus shows the transition between the Bloch and Debye limits with increasing H_{rf}. Note that for $|\gamma|H_{rf}T>3.5$, χ''/χ_0 undulates gently with the Debye value 0.33 as an asymptote.
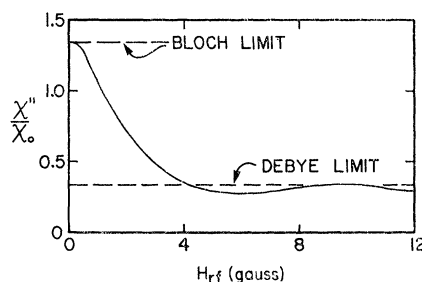
FIG. 2. Curve computed from modified Bloch equations showing the rf susceptibility χ'' in units of the static susceptibility χ_0 for $T_1=T_2=T=60$ nsec, $H_0=2.5$ G and a frequency of 7.0 Mc/sec.

The period ΔH_{rf} of oscillation of χ''/χ_0 was roughly the same as for δ_S in the case $H_0=0.5$ G and $f=7$ Mc/sec. Thus, ΔH_{rf} appears to be independent of H_0. This value of ΔH_{rf} is very close to the period shown for δ_S at 7.25 Mc/sec by Hecht.[5]

The solid curves of Figs. 3 and 4 show that the oscillatory nature of δ_S as a function of H_{rf} appears to require $\omega T\gtrsim 1$. Figure 5 shows the variation of δ_S with frequency while other parameters are held fixed. This curve is oscillatory and has the additional noteworthy feature that δ_S attains a value considerably in excess of unity at about 15 Mc/sec.

IV. EXPERIMENTAL PROCEDURE

The dynamic nuclear polarization at low fields was measured by placing the sample in the desired dc field H_0 and ac field H_{rf} for a sufficient time to achieve a steady state. Then these fields were turned off, and the sample was subjected to a homogeneous dc field essentially at right angles to H_0. The nuclear polarization that was generated by the combination of ac and dc fields then precesses around the new dc field and
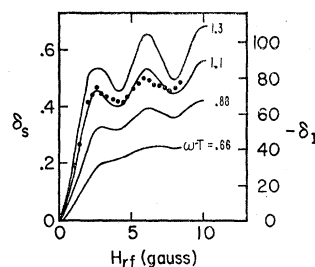
FIG. 3. Solid curves show electron spin saturation δ_S computed from the modified Bloch equations for a frequency of 3.5 Mc/sec, $H_0=0.5$ G, and $T_1=T_2=T=30$, 40, 50, and 60 nsec ($\omega T=0.66$, 0.88, 1.1, and 1.32, respectively). The experimental points represent the dynamic nuclear polarization plotted as δ_I, with a ratio of $k=-158$ between the δ_S and δ_I scales.

generates a signal in a suitable receiving coil, the signal being directly proportional in amplitude to the magnitude of the nuclear polarization.

The sample was a little less than a half-liter and was contained in a sealed cylindrical bottle. The bottle fits snugly into a solenoidal receiving coil with its common axis parallel to the earth's magnetic field. A small set of Helmholtz coils, having axis and center in common with the sample and the receiving coil, provides the required difference between H_0 and the earth's field.

The rf field was supplied by an elongated coil consisting of a few windings of copper tubing parallel to the axis of the receiving coil in a geometry which was a cylindrical analog of Helmholtz coils. The rf field was at right angles to H_0 and had an rms inhomogeneity of less than 5%. The rf field strength was measured by means of a large untuned pickup loop outside the receiving coil system. The output of the loop was rectified and measured with a voltmeter or oscilloscope. The large loop was calibrated by removing the sample and placing a small loop in various positions throughout the sample volume. The absolute calibration was accurate to within 7%. Relative field strengths could be read to about 2%. The final H_{rf} values were accurate to $\pm7\%\pm0.05$ G.
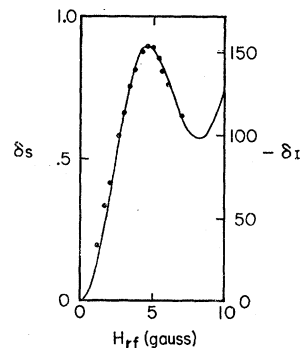
FIG. 4. Solid curve shows electron spin saturation δ_S computed from the modified Bloch equations for a frequency of 7.0 Mc/sec, $H_0=0.5$ G, $T_1=T_2=50$ nsec. The experimental points represent the dynamic nuclear polarization plotted as δ_I, with a ratio of $k=-172$ between the δ_S and δ_I scales.
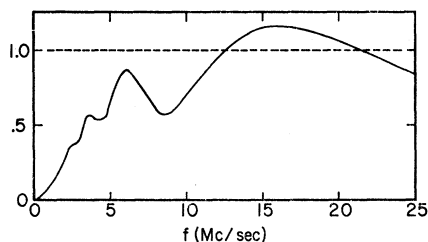
FIG. 5. Curve computed from modified Bloch equations showing electron spin saturation δ_S as a function of frequency for $H_{rf}=2H_1$ $=10$ G, $T_1=T_2=T=50$ nsec, and $H_0=0.5$ G.

The precession field H_{pr} was provided by a large set of Helmholtz coils with axis perpendicular to both H_{rf} and H_0.

The sequence of events for producing the signal was the following: (1) H_0 and H_{rf} were applied for a period of time of the order of a second (depending on the requirements of the particular sample). (2) After the current in the small coil (which produced H_0) had decayed to zero, voltages were applied simultaneously to both dc coils until the current in the large one reaches its final value to produce a field of about 1.5 G. (3) The current through the small dc coil is cut off suddenly. The field produced by the small dc coil builds up more rapidly and to a higher value, about 6 G opposed to the earth's field. The reason for the second energization of the small dc coil was that the field in the precession coil could not be built up fast enough to provide the "sudden" change in direction required for the desired precession of the polarization initially at right angles to it. The sudden change of direction of the resultant field was provided by the rapid cutoff of current in the small dc coil.

In addition to the steps described, some damping was applied to the receiving coil for a few milliseconds after the beginning of precession. The output of the receiving coil was amplified and displayed on an oscilloscope and photographed for measurement.

The method of producing and measuring dynamic polarization had the feature that, after a steady-state dynamic polarization was produced, the system of magnetic fields was returned to a standard configuration (earth's field) with no changes of direction. The nuclear polarization was parallel to the earth's field. Then a standard set of field manipulations produces a signal proportional to the polarization that was established. The possibility was avoided that the manipulation leading to precession could depend on H_0.

The unenhanced signal ($H_{rf}=0$) was proportional to H_0 and for weak fields was inferred from measurements with $H_0=40$ G. The signal-to-noise ratio was about ten for this field. The mean of a large number of measurements was used.

The ANI samples were made by dissolving anthracene in tetrahydrofuran, placing an excess of sodium metal in the solution, and sealing off the sample. Samples de-

teriorated rapidly if excess sodium was not left in the solution. In any case, samples deteriorated gradually over a period of months, as was easily checked by noting an increase in proton relaxation time (measured by low-field free-precession methods). The temperature for all measurements was $29\pm0.5°C$. The proton relaxation time was 50 msec.

V. EXPERIMENTAL RESULTS

Conventional electron resonance measurements at 3000 G and at 18 G gave values of the linewidth parameter $T_2=50$ nsec, each with accuracy better than 10%. Dynamic polarization measurements at a field of 18 G were made under resonant conditions using the apparatus of Poindexter.[11] From the saturation curve, the value $(T_1T_2)^{1/2}=50$ nsec was found, also with better than 10% accuracy.

Figure 3 shows the dynamic polarization data of the present experiment with $H_0=0.5$ G and $f=3.5$ Mc/sec plotted for $k=-158$, a value chosen for best fit to the curve computed for $T_1=T_2=T=50$ nsec, or $\omega T=1.1$. It is clear that even without independent knowledge of T, one can determine from the shapes of the computed curves that T must be close to 50 nsec. The fit of the data to the computed curve is strikingly close, but apparently not quite within known experimental uncertainties. The slightly less pronounced peaks and valleys of the experimental curve compared to the computed curve cannot be explained by time or space inhomogeneity of H_{rf}. The sample was not sufficiently conductive for significant shielding effect. It is not known whether or not an improved fit could be obtained by taking T_1 slightly different from T_2. However, a significant difference between T_1 and T_2 does not seem to be indicated even at the much higher field of the 18-G measurements. The signal-to-noise ratio for the highest readings was about ten. The points plotted are averages of five readings except for the lower points, where twenty readings are averaged. The relative values of the plotted points are thought to be accurate to within 5%. The scale of absolute values of δ_I is thought to be accurate within 5%.

Figure 4 shows the computed curve (for $T=50$ nsec) and experimental points for $H_0=0.5$ G and $f=7$ Mc/sec. The value $k=-172$ gave the best fit of experimental points to the computed curve. The relative accuracy is about twice as good as for the 3.5-Mc/sec data.

A value of k was determined, in addition, for resonant conditions at a somewhat higher frequency and field strength, namely, $H_0=5.0$ G, $f=14$ Mc/sec, and assuming $T=50$ nsec, the result is $k=-153$.

From the determinations under various conditions, there was no evidence that k was not a constant over the range of low-field conditions. Averaging the values ob-

[11] E. H. Poindexter, J. Chem. Phys. 37, 463 (1962).

tained and noting accuracy of the individual measurements, we arrive at a value of $k = -162 \pm 16$.

Thus, almost within the known experimental errors of the various measurements, the dynamic nuclear polarization of ANI can be computed from the modified Bloch equation [Eq. (1)] with $T_1 = T_2 = 50$ nsec and the Solomon relation [Eq. (6)] with $k = -162$ over a wide range of fields and under resonant and nonresonant conditions.

Some unexplained behavior was noted in an ANI sample which had deteriorated over a period of time. The time constant for the establishment of the steady-state dynamic nuclear polarization varied markedly with H_{rf} and was, in addition, much longer than T_1 for the proton spin system. It has been reported,[12] without knowledge of the sample deterioration, that this system did not respond according to both Eqs. (1) and (6), but this has now been attributed to sample deterioration.

One of the other solutions on which the low-field dynamic nuclear polarization measurements were made was a free-radical derived from crude oil, which was studied by Poindexter.[11] This particular radical is *not* exchange-narrowed, and its linewidth is hyperfine

[12] R. J. S. Brown and Don D. Thompson, Bull. Am. Phys. Soc. 8, 620 (1963).

broadened. For it, $T_1 > T_2 \cong 10$ nsec. Large signals were obtained from this solution with $H_0 = 0.5$ G as well.

A check was made of the effect of direction of the rf field. The coils producing H_{rf} were turned parallel to the dc field H_0. The ANI solution yielded absolutely no detectable "parallel" signal under conditions where the perpendicular fields gave a signal-to-noise ratio of nearly 50. This was expected from the MBE. However, Poindexter's radical solution yielded a "parallel" signal approximately one-third as large as the "perpendicular." We believe that this is due to the existence of unresolved hyperfine states in the radical, which would permit electron absorption between $m_F = 0$ components, where m_F is the total electron-plus-nucleus spin magnetic quantum number. These transitions are known to have parallel transition probabilities in weak dc fields.

We believe this transient dynamic nuclear polarization technique to be a very useful way to study electron relaxation behavior of solutions. First, large values of H_{rf} may be obtained at these low frequencies with conventional amateur transmitters; and second, the transient method avoids the troublesome rf heating problems encountered in continuous wave experiments. The rf is applied for only about 1 sec to fully polarize the nuclei.

Transverse and Longitudinal Optic Mode Study in MgF₂ and ZnF₂

A. S. BARKER, JR.

Bell Telephone Laboratories, Murray Hill, New Jersey

(Received 2 July 1964)

Infrared reflectivity measurements have been made on single-crystal MgF₂ and ZnF₂ in the wavelength range 1 to 140 μ. An analysis of the data using Kramers–Kronig analysis and classical dispersion theory gives the transverse optic mode frequencies, strengths, and linewidths. Huang's macroscopic dielectric theory is extended to the case of several modes to study the behavior of the longitudinal optic modes in these fluorides. A generalized Lyddane-Sachs-Teller relation and some additional sum rules are derived for the case of many modes when damping is present. It is shown that the longitudinal mode frequencies are easily obtainable from the reflectivity data analysis. The four longitudinal optic mode frequencies for MgF₂ and ZnF₂ are presented.

INTRODUCTION

MAGNESIUM fluoride and zinc fluoride are optically transparent insulators which crystallize with the rutile structure. This structure has space group $P4_2/mnm$ and point group D_{4h}. A group character analysis shows that these materials should exhibit three doubly degenerate infrared active modes with the electric vector perpendicular to the c axis and one nondegenerate infrared active mode with the electric vector parallel to the c axis.[1] At the present time the frequencies of these modes have not been established. A recent report by Hunt et al. describes reflection

experiments done on polycrystalline MgF₂.[2] Since reflectivity is a nonlinear function of the dielectric constant, analysis of average reflectivity does not yield an average dielectric constant for noncubic crystals. Thus the analysis carried out by Hunt et al. yields some incorrect frequencies and mode symmetries. Recent experiments performed by Johnson et al. on nickel- and cobalt-doped MgF₂[3,4] and cobalt-doped ZnF₂ have

[1] P. S. Narayanan, J. Indian Acad. Sci. 32A, 279 (1950).

[2] G. R. Hunt, C. H. Perry, and J. Ferguson, Phys. Rev. 134, A688 (1964).

[3] L. F. Johnson, R. E. Dietz, and H. J. Guggenheim, Phys. Rev. Letters 11, 318 (1963).

[4] L. F. Johnson, R. E. Dietz, and H. J. Guggenheim (to be published).